MOLECULAR AND CELLULAR BIOLOGY, Aug. 2002, p. 5887–5896 Vol. 22, No. 16
0270-7306/02/$04.00+0 DOI: 10.1128/MCB.22.16.5887–5896.2002

Mice Lacking Skeletal Muscle Actin Show Reduced Muscle Strength and Growth Deficits and Die during the Neonatal Period

K. Crawford,[1] R. Flick,[1] L. Close,[1] D. Shelly,[2] R. Paul,[2] K. Bove,[3] A. Kumar,[1] and J. Lessard[1]*

Divisions of Developmental Biology[1] and Pathology,[3] Children's Hospital Research Foundation, and Department of Physiology, University of Cincinnati, College of Medicine,[2] Cincinnati, Ohio 45229

Received 27 August 2001/Returned for modification 22 October 2001/Accepted 17 April 2002

All four of the muscle actins (skeletal, cardiac, vascular, and enteric) in higher vertebrates show distinct expression patterns and display highly conserved amino acid sequences. While it is hypothesized that each of the muscle isoactins is specifically adapted to its respective tissue and that the minor variations among them have developmental and/or physiological relevance, the exact functional and developmental significance of these proteins remains largely unknown. In order to begin to assess these issues, we disrupted the skeletal actin gene by homologous recombination. All mice lacking skeletal actin die in the early neonatal period (day 1 to 9). These null animals appear normal at birth and can breathe, walk, and suckle, but within 4 days, they show a markedly lower body weight than normal littermates and many develop scoliosis. Null mice show a loss of glycogen and reduced brown fat that is consistent with malnutrition leading to death. Newborn skeletal muscles from null mice are similar to those of wild-type mice in size, fiber type, and ultrastructural organization. At birth, both hemizygous and homozygous null animals show an increase in cardiac and vascular actin mRNA in skeletal muscle, with no skeletal actin mRNA present in null mice. Adult hemizygous animals show an increased level of skeletal actin mRNA in hind limb muscle but no overt phenotype. Extensor digitorum longus (EDL) muscle isolated from skeletal-actin-deficient mice at day 2 to 3 showed a marked reduction in force production compared to that of control littermates, and EDL muscle from hemizygous animals displayed an intermediate force generation. Thus, while increases in cardiac and vascular smooth-muscle actin can partially compensate for the lack of skeletal actin in null mice, this is not sufficient to support adequate skeletal muscle growth and/or function.

Actin forms the core of the thin filaments that are found in essentially all eukaryotic cells. It is required for cellular functions ranging from the generation and translation of mechanical force via a sliding-filament mechanism involving myosin filaments to the formation of rigid structures such as those found in intestinal microvilli and stereocilia. The actin gene family in vertebrates is comprised of six closely related proteins that are expressed in complex developmental and tissue-specific patterns (17, 33). All six of the functional actin genes reside on different chromosomes. This multigene family appears to have arisen by duplication after the separation of the vertebrates and urochordates (11). Two nonmuscle actins, cytoplasmic β- and γ-actin, are found in nonmuscle cells, and four actins which are very similar to one another (skeletal, cardiac, vascular, and enteric actin) comprise the major isoforms found in the adult muscle types for which they are named.

The primary sequences of the six isoactins are very similar. The cytoplasmic actins differ from the muscle actins at about 25 of the 374 amino acid residues that make up their primary structure. These replacements are generally conservative and involve the first 5 residues at the amino terminus and about 20 other substitutions scattered throughout the molecule. The paucity of changes among the actins presumably is due to a need to preserve the multiple interactions that these proteins must faithfully carry out with a large number of other proteins. Notably, the primary structures of all six actins are completely conserved across species ranging from birds to humans, arguing that the primary structures of these actins have been maintained for specific functional purposes. This is underscored by the recent demonstration that mutations in cardiac and skeletal actin are associated with dominant genetic muscle disorders. Point mutations in cardiac actin have been associated with both familial hypertrophic cardiomyopathy (18, 21) and dilated cardiomyopathy (22). Likewise, mutations in skeletal actin can lead to an actin-based nemaline myopathy (20).

It has been proposed, based on modeling, that the muscle actin genes have evolved from the nonmuscle actin genes by substitutions that lead to conformational changes in the N terminus and the internal dynamics of the actin molecule (19). The four muscle actins display variations at only 10 of the 375 amino acid positions in the molecule. Cardiac actin differs from skeletal actin by only four residues, while enteric actin varies at five positions and vascular actin differs at seven positions. The N terminus varies among all four muscle actins and has been directly implicated in the binding of myosin (31) and troponin I (14). While the functional significance of these amino acid exchanges is unknown, members of our laboratory and others have speculated (10) that each muscle actin has evolved to be particularly suited for specialized functional roles in those cells in which they are expressed (see references 23 and 8 for reviews).

The actin genes are developmentally regulated. While each

* Corresponding author. Mailing address: Division of Developmental Biology, Children's Hospital Research Foundation, 3333 Burnet Ave., Cincinnati, OH 45229-3039. Phone: (513) 636-8308. Fax: (513) 636-4317. E-mail: james.lessard@chmcc.org.

of the muscle actins comprises the predominant isoform in the four major muscle types (enteric, vascular, skeletal, and cardiac) in adults, isoactin expression during embryogenesis is highly regulated and complex. During development, each of the muscle types undergoes a unique pattern of transitions in the actin isoforms that they express. In chicken skeletal muscle, vascular actin is the first muscle isoactin to appear in the myotome (7, 25). Shortly thereafter, vascular actin expression is down regulated and cardiac actin expression increases. Around the time of birth, cardiac actin expression is down regulated while skeletal actin expression is up regulated, and the latter remains the predominant isoactin expressed in adult skeletal muscle. A similar process occurs during cardiogenesis, with the early expression of vascular, skeletal, and cardiac muscle isoactins and a considerable decrease in the expression of vascular actin and skeletal actin by birth (24). Interestingly, there is a simultaneous and transient reappearance of cardiac actin and skeletal actin in postnatal skeletal and heart muscles, respectively (3). The significance of these transitions in actin gene expression during myogenesis remains to be determined.

Transgenic approaches have been used in our laboratory to examine the developmental and functional significance of the muscle actins. Expressing enteric actin (the only isoactin that is never present in the myocardium) in the mouse heart results in a hypodynamic but otherwise normal heart (10). Similarly, while mice that are null for cardiac actin generally die in the perinatal period, animals expressing enteric actin in their hearts under the control of the cardiac α-myosin heavy-chain promoter can survive to adulthood; however, their hearts are enlarged and extremely hypodynamic. Thus, while enteric actin can substitute for cardiac actin, the presence of enteric actin results in significant functional perturbations.

In the study presented here, we have begun to assess the functional and developmental relevance of skeletal actin by disrupting the murine skeletal actin gene in embryonic stem (ES) cells and generating mice that lack a functional skeletal actin gene. Mice lacking skeletal actin survive to birth but die in the early neonatal period, generally around day 4 to 6. Interestingly, there is an apparent compensatory response involving an increase in the levels of vascular and cardiac actin in null animals such that the total actin content is not reduced in skeletal muscle and normal sarcomeric arrays are present in newborn skeletal myocytes. However, by day 2, extensor digitorum longus (EDL) muscle lacking skeletal actin produces less force. The skeletal-actin-null animals also show marked growth retardation and appear to die from malnutrition.

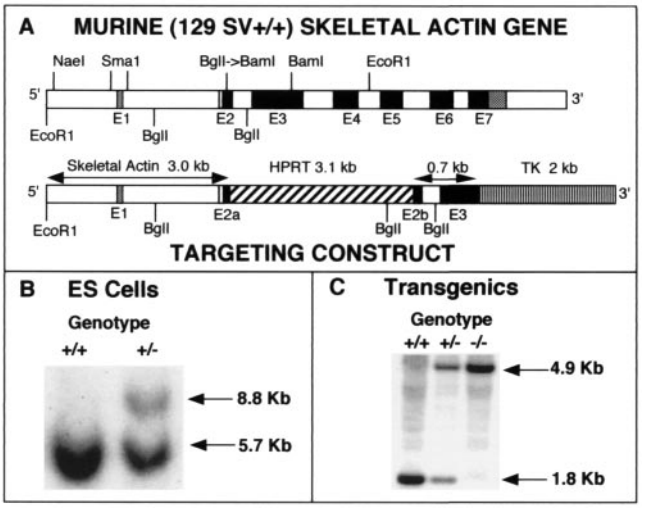

FIG. 1. Targeted disruption of the murine skeletal actin gene. (A) Targeting fragment. The exon-intron organization of the murine skeletal actin gene is shown at the top. Exons (E1 to E7) are represented by open boxes (noncoding exons) and dark boxes (coding exons). Details for the preparation of the targeting construct are presented in Materials and Methods. In brief, the *Bgl*I Site was converted to a *Bam*HI site by using the appropriate linker. The targeting construct was obtained by the ligation of an *HPRT* minigene cassette into the new *Bam*HI site within exon 2, and a TK cassette was linked to the 3′ end of the targeting construct. (B) Southern blot pattern of targeted and untargeted ES cells, with *Eco*RI used to digest the DNA and with the use of an *Eco*RI-*Nae*I probe. Note that the targeting event generates an 8.8-kb fragment due to the inclusion of the 3.1-kb HPRT cassette within exon 2. (C) Southern blot pattern used to genotype mice carrying the disrupted skeletal actin allele(s). DNA was digested with *Bgl*II and probed with an *Sma*I fragment that is contained within the 3′ end of the targeting fragment (0.7 kb) shown in panel A. Note that the targeted allele displays a 4.9-kb fragment that lacks the normal skeletal actin gene due to the presence of the 3.1-kb HPRT sequences.

MATERIALS AND METHODS

Molecular cloning and generation of skeletal-actin-mutant ES cells and mice. A genomic clone including the entire murine skeletal actin gene was isolated from a lambda DASH II 129/SvJ genomic library (28). Southern analysis localized the mouse skeletal-actin-coding region to a 6.0-kb *Eco*RI fragment that was subcloned into the *Eco*RI site of the IBI30 vector (IBI, New Haven, Conn.) for subsequent manipulations. The targeting vector is schematically represented in Fig. 1A and contains a phosphoglycerate kinase-hypoxanthine phosphoribosyltransferase (PGK-HPRT) minigene inserted in exon 2 and a PGK-thymidine kinase(TK)-poly(A) cassette downstream of the genomic sequences for positive and negative selection, respectively. About 3 kb of the skeletal actin gene is upstream of the PGK-TK cassette and includes the 5′-flanking region, exon 1, intron 1, and a portion of exon 2. In addition, 0.7 kb of genomic sequence is present 3′ of the HPRT cassette and contains sequences that include the remaining portion of exon 2, intron 2, and part of exon 3 of the skeletal actin gene.

To make the targeting vector, it was necessary to generate two contiguous upstream fragments and a single fragment downstream of the HPRT sequence, since convenient restriction sites were not available. A 1.8-kb *Bgl*II fragment was isolated from pE14/IBI and subcloned to obtain pSkel1. The *Bgl*I site within exon 2 was converted to a *Bam*HI site by use of the appropriate linkers. A 1.9-kb *Nae*I-*Sac*I fragment was isolated from pE14/IBI and subcloned into pGEM-11Zf(+) to give pUP1. From pUP1, a *Sac*I-*Not*I fragment was isolated to constitute upstream fragment 1 (U1). The second upstream fragment was a 1.1-kb *Sac*I-*Bam*HI fragment (U2) included in pSkel1. To obtain the downstream fragment, a 0.7-kb *Bam*HI-*Nru*I fragment was cloned into pBC SK+ restricted with *Bam*HI and *Eco*RV to yield the construct pDN1. A PGK-HPRT minigene-containing fragment with flanking *Xba*I and *Bam*HI sites was generated by initially cloning a *Sal*I cassette containing the HPRT marker into a *Xho*I-restricted pGEM-11zf(+) vector (Promega) to give pH1. From pH1, an *Apa*I-*Sal*I fragment was obtained and ligated into similar sites in pIBI30 (IBI, New Haven, Conn.) to yield pH2. Finally, the 3.1-kb mini-HPRT fragment was released from pH2 by restriction with *Bam*HI and *Xba*I. The PGK-TK cassette was obtained as a 2.0-kb fragment. Initially, a TK cassette (Stratagene, La Jolla, Calif.) was cloned into pBC SK+ to obtain the construct pT1. A *Hin*dIII-*Xho*I fragment from pT1 was used for the final construct. In a six-fragment forced cloning, the following fragments were ligated together: a pGEM-11zf(+) vector cut with *Xho*I and *Not*I, the two upstream fragments (the *Not*I-*Sac*I-cut U1 fragment and the *Sac*I-*Bam*HI-cut U2 fragment), the mini-HPRT marker cut with *Bam*HI and *Xba*I, the downstream fragment (D1 cut with *Xba*I and *Hin*dIII), and the TK fragment cut with *Hin*dIII and *Xho*I. The integrity of the final construct was confirmed by extensive restriction analysis.

The targeting fragment was obtained by restriction with *Sfi*I and *Not*I and purified using the Geneclean II kit (Bio 101). The linearized targeting construct (5 nmol) was electroporated into HPRT-E14TG2a ES cells derived from 129/Ola blastocysts. The ES cells were subsequently cultured in the presence of 120 μM

hypoxanthine–0.4 μM L-aminopterin–20 μM thymidine and ganciclovir (Sigma Chemical Co., St. Louis, Mo.) as directed by the manufacturer. After confirmation of homologous recombination, three independent ES cell clones were selected for injection into C57BL/6 blastocysts (Jackson Laboratory, Bar Harbor, Maine). Male progeny with a high percentage of coat color chimerism were bred to Black Swiss females (Taconic, Germantown, N.Y.) to establish germ line transmission. All animal experimentation was performed in the Children's Hospital Research Foundation animal care facility in accordance with the guidelines of the National Institutes of Health.

Isolation and analysis of genomic DNA. DNA was isolated from ES cell clones grown to confluence in 24-well tissue culture plates. The wells were rinsed twice with phosphate-buffered saline, and the cells were incubated with 0.5 ml of lysis buffer (0.2 M sodium chloride, 5 mM EDTA, 100 mM Tris-HCl [pH 8.3], 0.2% sodium dodecyl sulfate [SDS], 100 μg of proteinase K per ml) for 1 h in a 55°C humidified incubator. Absolute ethanol (1 ml) was added to each well, and the plate was placed on an orbital shaker for 30 min. The ethanol was drawn off, and the plates were washed with 2 ml of 70% ethanol with shaking for 15 min. The precipitated DNA along with a small volume of ethanol was transferred to a microcentrifuge tube. The pellet was allowed to settle, and all but 50 μl of ethanol was drawn off. After the DNA was allowed to air dry, it was resuspended in 100 μl of Tris-EDTA.

DNA was isolated from tail biopsy specimens with the Puregene DNA isolation kit (Gentra System, Inc., Minneapolis, Minn.). Southern hybridization was carried out to confirm the targeting event in ES cells and to genotype the mice. DNA from ES cells was restricted with *Eco*RI, while DNA from tail biopsy specimens was restricted with *Bgl*II, electrophoresed on 1% agarose gels, and transferred to Genescreen Plus nylon membranes (Perkin-Elmer Life Sciences, Boston, Mass.). A 0.4-kb *Eco*RI/*Nae*I fragment upstream of the skeletal actin gene segment in the targeting construct was used to confirm homologous recombination. Subsequently, a 0.7-kb *Sma*I fragment internal to the targeting construct was used as a probe to determine genotypes. Both probes were labeled with [α-^{32}P]dATP with a High Prime DNA labeling kit (Roche Molecular Biochemicals, Indianapolis, Ind.). The blots were hybridized at 65°C, washed under conditions of high stringency, exposed either to Kodak XAR-5 film or to PhosphorImager screens, and analyzed on a PhosphorImager (Molecular Dynamics, Sunnyvale, Calif.).

Northern analysis. 33 Hind limbs of progeny from heterozygote crosses were dissected, quick-frozen in liquid nitrogen, and stored at −140°C. The tails from these mice were used for genotyping by Southern hybridization. The hind limbs of littermates (+/+, +/−, and −/−) were used for total RNA isolation by extraction with RNA STAT-60 reagent (Tel-Test "B," Inc., Friendswood, Tex.) used according to the instructions of the manufacturer. Fifteen micrograms of RNA was loaded onto a 2.2 M formaldehyde-1.1% agarose gel, electrophoresed, and transferred to a Biotrans nylon membrane (ICN Biomedical, Inc., Costa Mesa, Calif.). Appropriate RNA controls were included in the analysis. To check the integrity of the RNA, aliquots were electrophoresed and stained with ethidium bromide. After transfer, the blot was serially hybridized to probes consisting of end-labeled, isoform-specific, and glyceraldehyde phosphate dehydrogenase (GAPDH)-specific oligonucleotides. The compositions of prehybridization and hybridization solutions were as described previously (10). The blots were probed for skeletal actin, cardiac actin, vascular smooth-muscle actin, and enteric smooth-muscle actin mRNAs as described previously (10). Likewise, GAPDH was used as an internal standard for sample loading. After each of the hybridizations described above, the blot was exposed to Kodak XAR-5 film. The bound probe was removed by washing the blot with a boiling solution of 0.1% SDS. Removal of the probe was confirmed before the next hybridization was carried out.

Western blotting. Newborn hind limbs were obtained and stored as described above (see "Northern analysis"). After genotyping was completed, the hind limbs from +/+, +/−, and −/− littermates were used for Western blotting. The hind limbs were homogenized in 100 μl of phosphate-buffered saline, SDS was added to the supernatant to a final concentration of 0.1%, and the tissue debris was removed by centrifugation. The sample was vortexed for 45 s, placed in a boiling water bath for 2.5 min, and centrifuged at 10,000 × *g* for 2 min, and the supernatant was then transferred to a fresh tube and used for Western blotting. Protein was measured by the Bradford method (2a). Samples of total limb protein (5 μg) were fractionated by SDS-polyacrylamide gel electrophoresis and electroblotted onto nitrocellulose membranes (Schleicher & Schuell Inc., Keene, N.H.). Total actin was detected with the monoclonal antibody (MAb) C4 (15), muscle actins were detected with MAb HUC 1-1 (25), vascular smooth muscle actin was detected with MAb 1A4 (29), enteric smooth muscle actin was detected with MAb B4 (25), and cardiac and skeletal actins were detected with MAb 5C5 (26). Antibody binding was detected with the Vectastain ABC system (Vector Laboratories, Inc., Burlingame, Calif.).

Morphological analyses. For morphological analyses, complete litters of newborn mice were sacrificed on day 1 or between days 4 and 6 and genotyped. Each litter included one or more examples of +/+, +/−, and −/− mice. Histochemical studies were performed on entire litters. The ultrastructures of skeletal muscles were determined on selected mice representing each genotype.

Fiber type analysis. For newborn mice (day 1), the hind limbs were disarticulated at the knee, mounted perpendicular to the long axis of the limb in gum tragacanth on cork slices, covered with talc to facilitate rapid freezing, and then quick-frozen in liquid nitrogen. Cryostat-generated sections were stained with hematoxylin and eosin or by the modified Gomori trichrome method. Sections were stained for myosin ATPase activity after preincubation in substrate at pH 4.3, 4.6, and 10.0. When neonatal mice were studied (days 4 to 6), the hind limbs were disarticulated at the hip, mounted, and studied as described above.

Electron microscopy. The EDL muscle was sampled in newborn (day-1) mice. Muscle of the upper thigh was sampled in newborn mice at sacrifice on days 4 to 6. Muscle samples were minced in 2% glutaraldehyde buffered with 0.175 M cacodylate, postfixed in osmium tetroxide, dehydrated in graded alcohol, and embedded in epoxy resin. Ultrathin sections were stained with uranyl acetate-lead citrate and examined with a Zeiss 912 electron microscope.

Whole-body mounts. The trunks of the newborn mice were fixed in formalin. Coronal sections, 2 mm thick, were processed into paraffin, and 5-μm-thick sections were stained with hematoxylin and eosin; the periodic acid-Schiff stain method was also used alone and after diastase digestion to remove glycogen.

Muscle physiology. Neonatal EDL muscles were removed to measure contractility and muscle mechanics at 2 to 3 days of age. Neonates were euthanized by decapitation. EDL muscles were surgically exposed, and the resting length of each muscle was measured in situ. Muscles were removed with tendons intact and maintained at resting length at all times during the experiments by using suture silk. Muscles were mounted in a small, constant-temperature, sealed chamber. Muscles were fixed at one end to a stationary stainless-steel post by using suture silk. The other end was fixed to the lever of an isometric force transducer via a thin glass rod and adjusted to resting tension. Muscles were kept in sterile Krebs solution (236 mM NaCl, 9.46 mM KCl, 50 mM $NaHCO_3$, 5 mM $CaCl_2$, 2.38 mM $MgSO_4$, 1.16 mM NaH_2PO_4, 0.26 mM EDTA equilibrated with 95% CO_2-5% O_2) at 37°C.

Muscles were electrically field stimulated to a state of fused tetanus via platinum wire electrodes with capacitor discharges of equal but alternating polarity (66 to 80 Hz at 12to 25 V). Experiments consisted of a set of instances (5 to 10) of fused tetanus, with tetanus duration (3 to 14 s) determined randomly. Individual instances of tetanus from digitized records of force production obtained with a data acquisition system (BioPac System, Inc., Goleta, Calif.) were evaluated to determine maximal tetanic tension.

RESULTS

Targeted disruption of the skeletal actin gene. To disrupt the skeletal actin gene in ES cells, a targeting vector was constructed in which an *HPRT* minigene was placed in exon 2 at a position corresponding to amino acid residue 19 in mature skeletal actin. The HPRT cassette was flanked upstream by 3 kb of sequence from the skeletal actin gene, and 0.7 kb of the skeletal actin gene was included downstream (Fig. 1A). A TK cassette was located at the 3′ end of the targeting vector to enhance selection of homologous recombinants. After electroporation into E14TG2a ES cells and selection in 120 μM hypoxanthine–0.4 μM L-aminopterin–20 μM thymidine and ganciclovir, 178 clones were screened for the targeting event by Southern blotting (Fig. 1B), and 6 clones tested positive. Each clone showed a single site of integration of the targeting fragment into the mouse genome.

Three independent clones were used for injection into blastocysts to generate chimeras. Two male chimeras from an ES cell clone designated LES78 showed germ line transmission when they were outbred to NIH Black Swiss females (Fig. 1C). All of the animals described here were of this mixed genetic

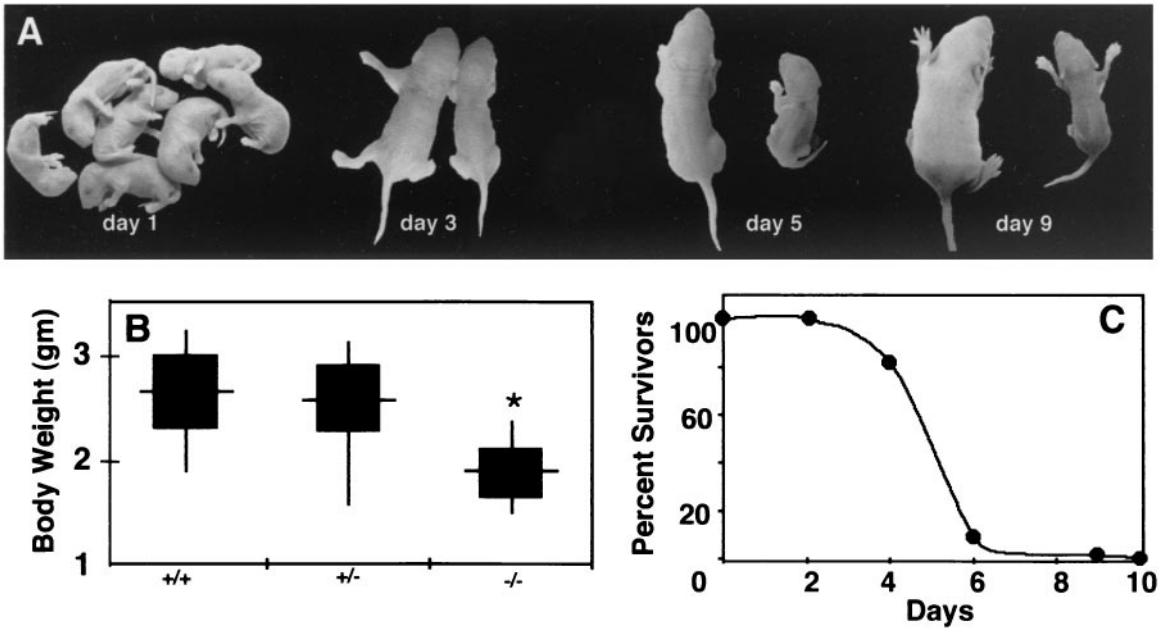

FIG. 2. Skeletal-actin-null mice do not survive the neonatal period and show marked growth retardation. (A) Homozygous null mice appear normal at birth but fail to thrive. Littermate pairs are shown at the ages indicated, with the wild-type mouse on the left and the skeletal-actin-null mouse on the right for each pair. While all pups appeared normal at birth, by day 3 and beyond, the skeletal-actin-deficient animals were clearly smaller than normal. Note the scoliosis in the day-5 skeletal-actin-null mouse. (B) Comparison of the body weights of normal (+/+), hemizygous (+/−), and homozygous (−/−) null mice 4 days after birth. The data are presented as the range (vertical line), mean (horizontal line), and standard deviation (black box). The genotypes of newborns from four litters of heterozygote mutings showed a Mendelian distribution: 11 +/+, 24 +/−, and 10 −/−. (C) Survival of skeletal-actin-null mice. Six litters consisting of 57 animals were monitored for 10 days. By day 6, only 1 of 11 homozygous null animals was alive, while 91% of the wild-type animals and 85% of the heterozygous null pups were alive.

background. Skeletal actin +/− mice were phenotypically normal and fertile.

Mice deficient for skeletal actin die as neonates. When skeletal actin heterozygotes were bred, the initial F_2 litters contained a typical Mendelian distribution of offspring. Null mice were indistinguishable from wild-type mice or heterozygous littermates at birth (Fig. 2A). However, skeletal-actin-deficient mice were significantly smaller by 4 days of age (Fig. 2A and B). Within 3 to 4 days after birth, homozygous null mice showed significantly lower body weights than wild-type or heterozygous littermates (Fig. 2B). The null mice also frequently displayed signs of scoliosis that are consistent with muscle weakness (Fig. 2A). As shown in Fig. 2C, all skeletal-actin-null mice died within 10 days of birth and most died between 4 and 6 days after birth.

Skeletal actin depletion results in increased levels of vascular smooth-muscle actin and cardiac actin in skeletal muscle. The fact that skeletal-actin-null mice can breathe and move their limbs indicates that their skeletal muscles are functional in spite of an absence of skeletal actin. To determine if this is due to a compensatory increase in other actins as observed in cardiac-actin-knockout mice (10), we examined the isoactin composition of skeletal muscle from mice of the three genotypes at the mRNA (Fig 3) and protein (Fig 4) levels.

Northern analysis of the limbs from skeletal actin −/− mice on day 3 showed an absence of skeletal actin mRNA (Fig. 3). Both vascular smooth-muscle and cardiac actin mRNA levels are increased in the skeletal-actin-null limbs (Fig. 2B) relative to limbs from wild-type mice. The mRNA levels of all three of these muscle actins also increased in the heterozygous null animals, but no enteric actin mRNA was detected in any of the samples (data not shown). Quantification of the Northern blot data from +/− muscle with ImageQuant software showed an approximately 50% increase in skeletal actin mRNA. Both +/− and −/− muscle showed approximately 75% increases in

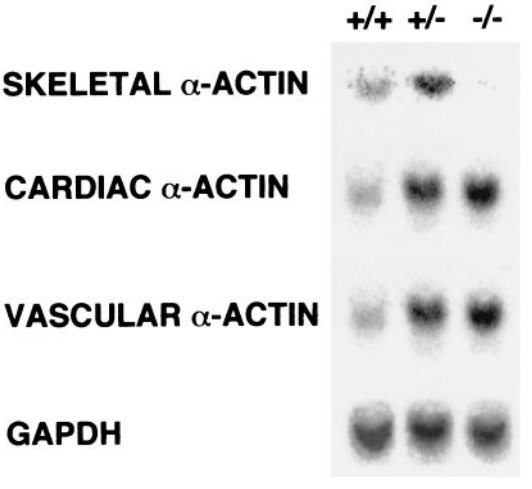

FIG. 3. Muscle actin mRNA content of limbs from wild-type (+/+), hemizygous (+/−), and homozygous (−/−) null mice 3 days after birth. GAPDH mRNA levels were also determined as an internal standard for loading.

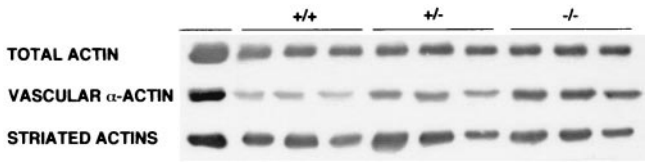

FIG. 4. Actin content of limbs from wild-type (+/+), hemizygous (+/−), and homozygous (−/−) null mice 3 days after birth. Three separate samples were assayed by immunoblotting. Total actin levels were assessed with MAb C4, vascular actin levels were determined with MAb 1A4, and striated actins (skeletal actin plus cardiac actin) were measured with MAb 5C5, as described in Materials and Methods.

both cardiac and vascular smooth-muscle actin mRNA levels relative to the levels of these mRNAs in +/+ muscle. Interestingly, the converse compensatory response was observed in the hearts of cardiac-actin-deficient animals; that is, skeletal actin mRNA and vascular actin mRNA were elevated in the hearts of mice that were either heterozygous null or homozygous null for cardiac actin, and again, no enteric actin was detected (10). Similarly, the level of cardiac actin mRNA was elevated in the hearts of heterozygous null animals.

At the protein level, there is no significant difference in total actin content among +/+, +/−, or −/− muscles when normalized to total protein (Fig. 4), as demonstrated by immunoblotting with MAb C4, which recognizes an epitope shared by all actins (15). Likewise, the total amount of striated actin (cardiac plus skeletal actin) is approximately the same based on immunoblots with MAb 5C5. However, since no skeletal actin is present in the −/− muscles, this signal must represent cardiac actin. Vascular smooth-muscle actin, detected with MAb 1A4, increases by about 50% in skeletal actin (+/−) and almost threefold in −/− leg muscle. Enteric smooth-muscle actin clearly is not involved, since this protein was not detected with MAb B4 (data not shown).

In combination, the results demonstrate that the gene-targeting strategy used here generated a null mutation in the skeletal actin gene. Moreover, the data indicate that there is a compensatory response to decreased levels of skeletal actin in neonatal muscle involving the increased accumulation of vascular smooth-muscle actin and cardiac actin.

Newborn null mice show normal muscle fiber maturity and size. Histological analysis (Fig. 5) surveying muscles of the trunk, upper thigh, and upper foreleg suggests that there is little difference in muscle fiber maturity or fiber size between null and wild-type newborn animals. Prominent interstitial space, suggestive of immaturity, was more prevalent in the muscles of null mice. At birth, there is a wide variation among muscle groups with regard to the extent of muscle fiber maturation, as reflected by such indexes as the frequency of central nuclei and the pattern of myofiber subtypes detected by the myosin ATPase reaction. This variability is apparent in Fig. 5, and no consistent difference was observed between the null and wild-type mice in frozen sections from comparable regions.

Importantly, the ultrastructure of myofibrils and sarcomeres of wild-type and null animals was normal in newborn muscle with respect to the appearance and integration of thin filaments at the Z, I, and A bands (Fig. 6A). Furthermore, the typical hexagonal arrangement of thin and thick filaments is evident (Fig. 6B).

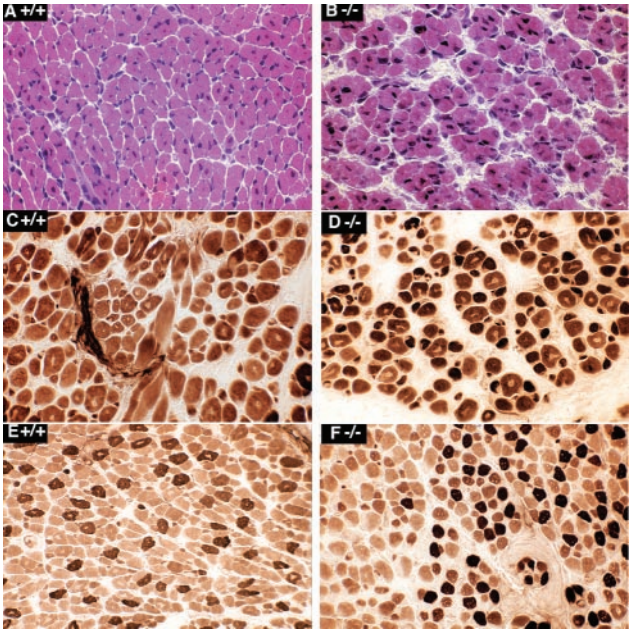

FIG. 5. Thigh muscles of 1-day-old wild-type (+/+) mice (A, C, and E) and homozygous null (−/−) mice (B, D, and F) show no consistent differences in myofiber diameter range, frequency of central nuclei (a feature of immaturity), or myofiber subtype differentiation. Central nuclei are common in panels B, C, D, and E. Mature fiber subtypes are present in panels E and F. The ranges of fiber diameter are similar in all panels; however, the intercellular space is greater in the −/− samples. Panels A and B are sections that were stained with hematoxylin and eosin, while panels C, D, E, and F are sections that were stained for myosin ATPase following incubation at pH 4.6, as described in Materials and Methods.

Skeletal-actin-null animals appear to die from malnutrition. At 4 days of age, null animals exhibited severe atrophy of brown fat, severe depletion of glycogen stores in hepatocytes and skeletal muscle fibers, and reduced muscle fiber diameter compared to littermate controls (Fig. 7). Quantitative comparison of muscle fiber diameter in paraspinal muscles revealed a 17% reduction in the starved animals. A severe reduction in intermyofibrillar glycogen granules was also observed in electron micrographs of skeletal muscle from null animals but not of that from wild-type mice (Fig. 6). Thus, by 4 days after birth, the null mice showed signs of severe postnatal malnutrition that appeared to be the cause of their death within the next few days.

Force production in null muscles is lower than that of wild-type muscles. To test muscle function, we developed a method to electrically stimulate and measure contractility in muscle preparations from newborns. Due to the small size of these muscles, accurate weights were difficult to obtain and thus we normalized the tension data to muscle length. No significant differences were observed in the mean length of the neonatal EDL muscles from 1-day-old wild-type (4.14 ± 0.13 mm [mean ± standard error of the mean]), hemizygous (3.85 ± 0.20 mm), and homozygous null (3.97 ± 0.22 mm) mice. When this normalization routine was used, the peak force was significantly lower in the homozygous null muscles than in wild-type muscles, while heterozygous muscles showed intermediate force production (Fig. 8). Two other

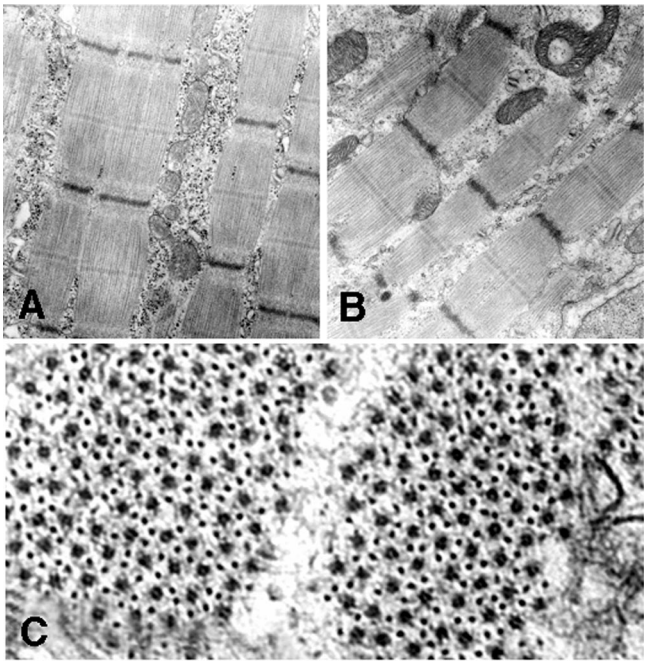

FIG. 6. Newborn leg muscle was examined by electron microscopy as described in Materials and Methods. (A and B) A comparison of wild-type muscle (A) and skeletal-actin-null muscle (B) indicates that thin- and thick-filament organization of sarcomeres appears normal in homozygous null (−/−) mice at 1 day of age. (C) Cross-section of muscle of a skeletal-actin-null mouse showing the normal hexagonal organization of thick and thin filaments. Note that glycogen granules are depleted in the muscle sample from the null mouse.

normalization routines were evaluated: force normalized to body weight and force normalized to muscle length divided by body weight (which reflected an attempt to approximate the muscle cross-sectional area assuming scaling of muscle weight with body weight). In all cases, plots of the data from the additional normalization routines, in addition to raw tension data, show similar trends, with the muscles of null animals producing significantly lower force than those of the wild-type mice and those of the hemizygous mice producing intermediate levels of force.

DISCUSSION

Most of the myofibrillar proteins exist in multiple isoforms, and virtually every contractile protein undergoes at least one isoform transition during the normal course of muscle development. In addition to actin, these multigene families include the myosin heavy and light chains, tropomyosin, troponin, and C-protein. Thus, the four major types of adult muscle (skeletal, cardiac, vascular, and enteric) contain tissue-specific isoforms of many of these components, and they share others. The functionally and biochemically distinct contractile structures found in different cells (e.g., nonmuscle, smooth muscle, and striated muscle) are believed to result from the specific complement of cytoskeletal and contractile elements expressed in a particular cell type. However, with the possible exception of the myosins, the exact physiological significance of the developmental transitions in many of these proteins, including the actins, is poorly understood.

During development, each of the different muscle types (enteric, vascular, cardiac, and skeletal) undergoes highly regulated transitions in the expression of actin isoforms. In skeletal muscle, where actin expression has been studied extensively, vascular actin is the first muscle isoactin to be expressed during myogenesis (7, 16, 17). Shortly thereafter, vascular actin expression is down regulated and cardiac actin expression increases. Around the time of birth, cardiac actin expression decreases while skeletal actin expression increases and then remains the predominant isoactin in adult skeletal muscle. Cardiac actin and skeletal actin reappear in skeletal muscle and heart muscle, respectively, 2 to 3 weeks after birth.

To assess the functional and developmental significance of skeletal actin, we generated skeletal-actin-deficient mice. In this report we show that skeletal-actin-deficient (−/−) mice are indistinguishable from normal mice at birth in terms of size, but they fail to thrive and thus die in the neonatal period. Although the null animals can breathe, walk, and suckle, apparently through a compensatory response leading to an increased expression in their skeletal muscles of cardiac and vascular actin, their muscles are weaker than those of their hemizygous and wild-type littermates and they die within 10 days, apparently from malnutrition.

Phenotypic effects of loss of skeletal actin. Skeletal actin comprises about 90% of the muscle actin in adult mouse skeletal muscle. However, significant levels of cardiac actin are found in fetal and neonatal muscle, where it can comprise up to 50% of the total actin (32). In response to the absence of skeletal actin, both vascular actin and cardiac actin mRNA levels are increased in neonatal muscle (Fig. 3). Importantly, vascular smooth-muscle actin comprises only a minor component of normal skeletal muscle (25), and it is not likely that this contributes significantly to the total actin pool even though it increases by about 50% in the leg muscle of skeletal-actin +/− animals and by almost threefold in that of −/− animals. Enteric smooth-muscle actin clearly is not involved, since this protein was not detected with MAb B4 (data not shown). This is consistent with earlier reports that enteric actin is never expressed in normal rodent skeletal muscle cells (17, 25). Thus, the principal actin in the limb muscles of skeletal-actin-null newborns appears to be cardiac actin.

Similar compensation phenomena involving increases in alternative actin forms have been shown in several other situations. For example, expression levels of both skeletal actin and vascular smooth-muscle actin are increased, the former transiently, following work overload-induced hypertrophy in the adult rodent heart (2, 9, 27). Likewise, in the adult BALB/c mouse heart, there is a reduced level of cardiac actin associated with a 9.5-kb duplication of a part of the cardiac actin gene that results in the increased expression of skeletal actin (3, 15). Furthermore, we have reported that cardiac-actin-null mice show increases in skeletal and vascular actin in their hearts (10). Interestingly, neonates that are hemizygous for the skeletal actin gene show enhanced levels of vascular smooth-muscle actin and cardiac actin as well as skeletal actin mRNAs. A similar response was observed in the hearts of newborn mice that were hemizygous for the cardiac actin gene. In combination, these studies suggest that all three actins (cardiac, skeletal, and vascular) play a role in actin homeostasis in developing skeletal and cardiac muscle.

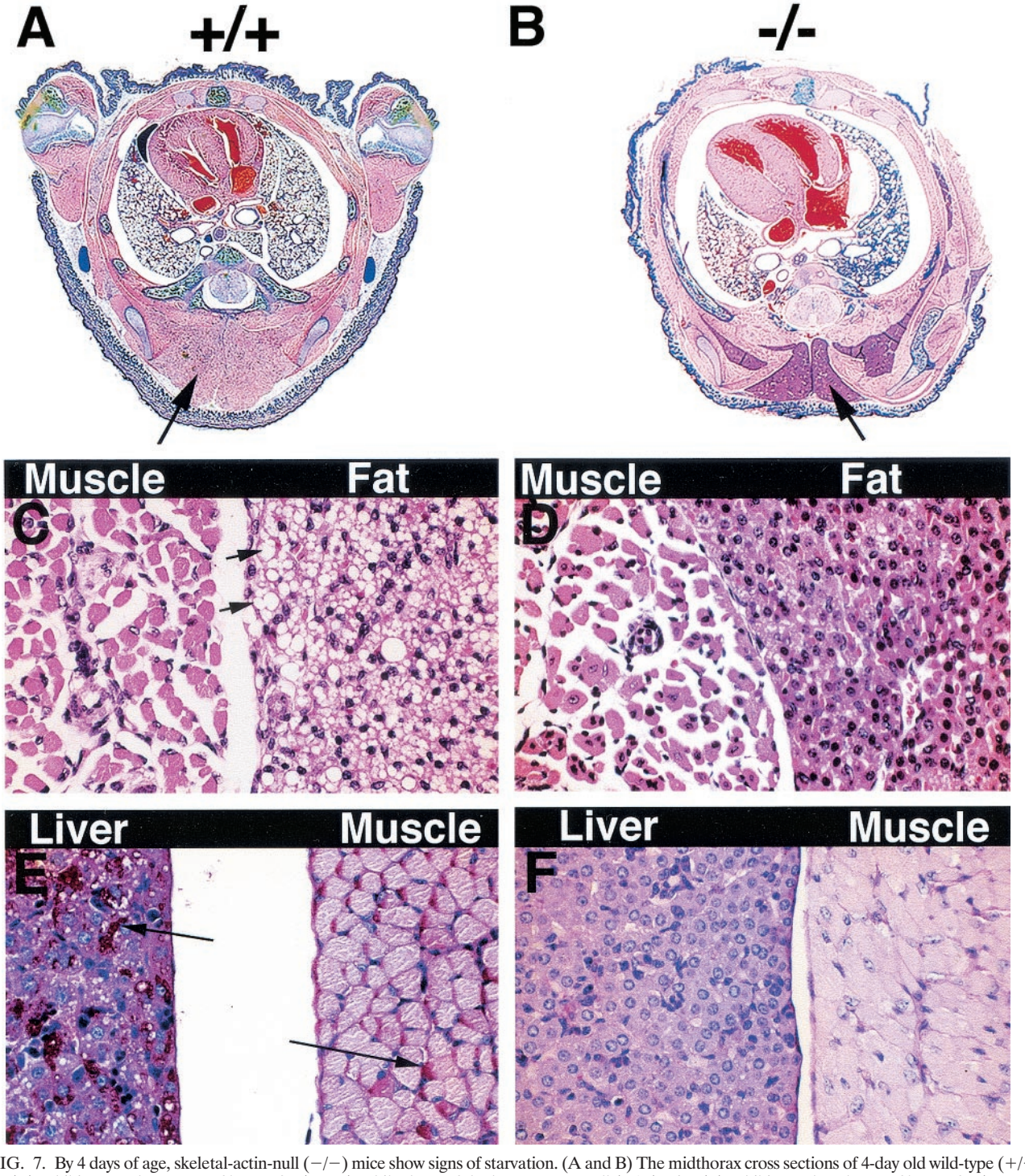

FIG. 7. By 4 days of age, skeletal-actin-null (−/−) mice show signs of starvation. (A and B) The midthorax cross sections of 4-day old wild-type (+/+) mice (A) exhibit normal amounts of brown fat (arrow), while those of the homozygous null (−/−) mice (B) exhibit a reduced area of brown fat (arrows). (D and E) Microscopic details demonstrate that homozygous null mice (D) had markedly less lipid (small arrows) in brown fat cells than wild-type animals (C) did. Similarly, there is a marked depletion of both liver and muscle glycogen in homozygous null mice (F) relative to wild-type mice (E); i.e., the magenta-colored grains corresponding to glycogen (large arrows) are abundant in panel E and absent in panel F. Note the smaller paraspinal muscle fibers with more frequent central nuclei found in null mice (D) at this age relative to those in wild-type mice (C). Panels C and D are sections that were stained with hematoxalin and eosin; panels E and F are sections that were stained for glycogen with periodic acid-Schiff stain.

The hind limb muscles of newborn mice that are null for skeletal actin do not differ from those of normal littermates in terms of size and fiber types. However, skeletal-actin-null mice fail to grow beyond birth. Normally, there is significant growth of existing muscle fibers, along with the addition of nuclei by fusion with mononucleated precursor cells or satellite cells in the postnatal period. There are also large increases in both the diameter and the length of fiber due to postnatal increases in

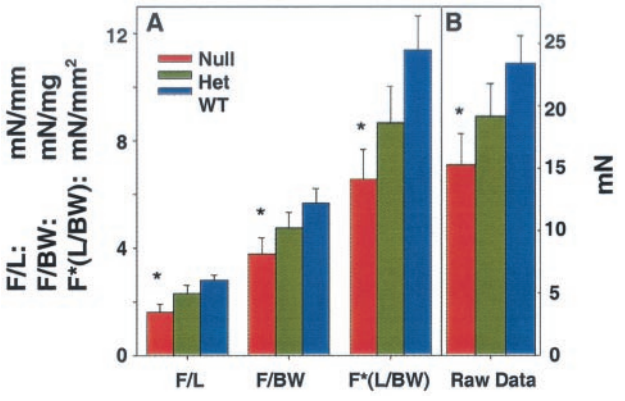

FIG. 8. EDL muscle from 1- to 2-day-old skeletal-actin-null (−/−) mice shows a reduced maximum tetanic tension. (A) Measurements of maximal force from electrically stimulated neonatal wild-type (+/+) (WT), heterozygous (+/−) (Het), or homozygous null (−/−) (Null) EDL muscles. Measurements were normalized to muscle length (F/L, in millinewtons per millimeter), body weight (F/BW, in millinewtons per milligram), or muscle length divided by body weight (F∗[L/BW], in millinewtons per square millimeter), where F represents force, L represents length, and BW represents body weight. (B) Raw data for measurements of force produced by maximally electrically stimulated EDL muscles (in millinewtons). In all cases, the skeletal-actin-null (−/−) muscle produced significantly less force than +/+ muscle, while (+/−) EDL muscles are intermediate. All values are means ± standard errors of the mean. Asterisks indicate results that are significantly different from values for the wild-type mice at $P < 0.05$ via t test.

the number of myofilaments per fiber. The basis for the failure of skeletal-actin-deficient animals to thrive remains to be determined but is most likely due to an insufficient amount of muscle actin. Alternatively, the increased levels of cardiac actin and/or vascular actin may inhibit the growth of skeletal-actin-null muscles. Gunning et al. (6) have shown that the expression of skeletal actin, but not cardiac actin, has a profound effect on C2 myoblast morphology. Thus, the lack of growth in skeletal-actin-deficient cells may be due to quantitative and/or qualitative effects because of changes in the actin content of skeletal muscle.

Considering the nature of the gene alteration in these animals and the fact that this alteration was lethal, we were interested in assessing the contribution of contractile function to the lethality of this condition. We chose the EDL muscle as a representative fast-twitch muscle both for its relative ease of dissection and for its relatively uniform shape. In the present study, we observed a significant reduction in the ability of the EDL muscles of homozygous null mice to produce force compared to those of wild-type mice, with those of hemizygous mice being intermediate. Several explanations for the loss of force production can be postulated. The simplest explanation is that the ratio of actin to myosin has been reduced, resulting in the formation of fewer cross bridges for any given level of contractile stimulation and hence in lower force. While quantification of the number of total actin filaments is difficult, the sarcomeric organization of skeletal muscle appears normal at birth.

Given the conserved nature of skeletal muscle actin, it is also conceivable that the interaction of skeletal actin with skeletal muscle myosin may be fundamentally different from that of vascular actin or cardiac actin. Members of our laboratory have shown previously that the substitution of cardiac actin by enteric actin results in an enlarged and hypocontractile heart (10). Similarly, enteric actin has been shown to have a reduced affinity for skeletal muscle myosin (30). However, similar studies have not demonstrated differences in the ability of cardiac actin to activate skeletal muscle myosin ATPase. Such studies have not been carried out with vascular actin, since the interpretation would be complicated by the fact that vascular smooth muscle also contains variable amounts of enteric actin and nonmuscle actins.

As noted above, the ratio of cardiac to vascular actin in the EDL muscles of homozygous null animals is unknown, but it is likely that cardiac actin predominates. In any event, it is known that myosin isoforms in the heart and vascular smooth muscle that interact with cardiac and vascular actin are biochemically and structurally different from those found in skeletal muscle. Furthermore, while the mechanism regulating the interaction of actin and myosin in cardiac muscle is similar to that of skeletal muscle, this mechanism differs significantly in vascular smooth muscle. Contractility in vascular smooth muscle is modulated via a Ca^{2+}-calmodulin activation of myosin light-chain kinase rather than the binding of Ca^{2+} to the troponin/tropomyosin complex. These variations in the regulation of cross bridge formation may result in a mismatch of vascular and cardiac actin with skeletal-muscle myosin, resulting in the reduced capability for force production that we observed. Additionally, we cannot discount the possibility that the expression of cardiac or vascular actin fundamentally altered the expression of skeletal muscle myosin isoforms from fast-twitch to slow-twitch fibers. However, this is unlikely, as changes in skeletal-muscle myosin typically occur over days or weeks rather than so soon after birth. It is also possible that undetermined compensatory biochemical or structural changes in skeletal muscle result in a weaker muscle in skeletal-actin-null animals.

Regardless of the mechanism, we hypothesize that the reduced force production in the skeletal muscle of homozygous null animals contributes to a reduced capability to mobilize and to a competitive disadvantage during feeding, preventing the null mice from obtaining adequate caloric intake. At the time of death, null animals exhibited severe atrophy of brown fat (Fig. 6A), severe depletion of glycogen stores in liver (Fig. 6B), muscle immaturity, and reduced skeletal muscle fiber diameter compared to controls. A severe loss of glycogen granules in muscle was also apparent. Thus, the null mice showed signs of severe postnatal malnutrition, presumably due to general skeletal muscle deficit, that ultimately resulted in their death. Goldspink and Rowe have examined the response of muscle to partial starvation (5). Starvation did not affect the total number of fibers or the numbers of any fiber type, but food deprivation prevented the growth of muscle, as normally reflected by an increase in the DNA content of the skeletal muscle of young rats. Rather, total DNA remained constant in food-deprived animals, while muscle weight and RNA content decreased. They observed that high-ATPase fibers showed the greatest decrease in size. Of these, the ATPase-high glycolytic type responded more than the ATPase-high oxidative type. Since the effects of the undernutrition on the different fiber types were found to be completely reversible, we attempted to

separate the presumptive skeletal-actin-null animals from larger littermates to reduce competition, but this did not enhance their survival. Interestingly, mice lacking myosin heavy-chain IId or myosin heavy-chain IIb show reduced body weights relative to normal mice; animals which are null for either of these myosins appear to survive to adulthood due to the up regulation of myosin heavy-chain IIc (1). Just as with skeletal-actin-null mice, about one-third of the myosin heavy-chain IId-deficient mice show kyphosis as neonates; however, none of the mice which were null for myosin heavy-chain IIb showed evidence of scoliosis or kyphosis.

Since striated muscle is a tissue in which gene expression is influenced to a large extent by mechanical signals, the reduced strength of the skeletal-actin-null mice may be expected to have more global effects. However, based on our results, this does not include the determination of muscle fiber phenotype, which depends on which protein isoform genes are transcribed. Rather, the effects appear to be principally on muscle fiber mass accretion, which in turn is likely to involve transcriptional and/or translational regulation. Clearly, these studies demonstrate that muscle has a remarkable ability to compensate, at least partially, by expressing different isoforms of the same protein.

The importance of the proper composition and function of both thick and thin filaments is underscored by the fact that several inherited muscle diseases have been associated with defects in various contractile proteins. For example, cardiomyopathy can be caused by mutations in cardiac actin, α-myosin heavy chain, troponin C, or tropomyosin. Likewise, nemaline myopathy in humans has been associated with mutations in three genes encoding sarcomeric thin filament proteins: skeletal actin (20), α-tropomyosin slow (12), and nebulin (13). Nemaline myopathy is highly variable in its clinical signs. For example, skeletal muscle weakness can be mild to severe and can show a slow progression such that patients may survive to adulthood. At the other extreme, a severely affected individual may die shortly after birth. Importantly, these thin-filament-based forms of nemaline myopathy almost always result from spontaneous mutations that exhibit a dominant recessive phenotype. In contrast, heterozygous mice that are null for either cardiac or skeletal actin show little or no phenotype and survive to adulthood. The lack of a haploinsufficiency phenotype further reinforces the notion that actin-based myopathies of both skeletal muscle and the heart result from functional effects caused by the mutant actin. These alterations have been hypothesized to affect the interaction of actin with myosin or other components of the contractile apparatus and may be subtle or severe. Corbett et al. (4) have expressed a dominant negative α-tropomyosin slow (Met9Arg) mutation specifically in skeletal muscle of mice by using two different promoters. They found that all features of the disease observed in human patients with this mutation are present in mice. Further experimentation involving the generation of animal models will be required to elucidate the mechanisms leading to actin-based nemaline myopathy.

ACKNOWLEDGMENTS

This work was supported by grants to J.L.L. from the Muscular Dystrophy Association and the NIH.

REFERENCES

1. **Allen, D. L., and L. A. Leinwand.** 2001. Postnatal myosin heavy chain isoform expression in normal mice and mice null for IIb or IId myosin heavy chains. Dev. Biol. **229:**383–395.
2. **Black, F. M., S. E. Packer, T. G. Parker, L. H. Michael, R. Roberts, R. J. Schwartz, and M. D. Schneider.** 1991. The vascular smooth muscle alpha-actin gene is reactivated during cardiac hypertrophy provoked by load. J. Clin. Investig. **88:**1581–1588.

2a. **Bradford, M. M.** 1976. A rapid and sensitive method for the quantitation of microgram quantities of protein utilizing the principle of protein-dye binding. Anal. Biochem. **72:**248–254.

3. **Collins, T., J. E. Joya, R. M. Arkell, V. Ferguson, and E. C. Hardeman.** 1997. Reappearance of the minor alpha-sarcomeric actins in postnatal muscle. Am. J. Physiol. **273:**C1801–C1810.
4. **Corbett, M. A., C. S. Robinson, G. F. Dunglison, N. Yang, J. E. Joya, A. W. Stewart, C. Schnell, P. W. Gunning, K. N. North, and E. C. Hardeman.** 2001. A mutation in alpha-tropomyosin (slow) affects muscle strength, maturation and hypertrophy in a mouse model for nemaline myopathy. Hum. Mol. Genet. **10:**317–328.
5. **Goldspink, G., and R. W. Rowe.** 1968. Studies on postembryonic growth and development of skeletal muscle. II. Some physiological and structural changes that are associated with the growth and development of skeletal muscle fibres. Proc. R. Ir. Acad. Sect. B **66:**85–99.
6. **Gunning, P. W., V. Ferguson, K. J. Brennan, and E. C. Hardeman.** 2001. Alpha-skeletal actin induces a subset of muscle genes independently of muscle differentiation and withdrawal from the cell cycle. J. Cell Sci. **114:** 513–524.
7. **Hayward, L. J., and R. J. Schwartz.** 1986. Sequential expression of chicken actin genes during myogenesis. J. Cell Biol. **102:**1485–1493.
8. **Herman, I. M.** 1993. Actin Isoforms. Curr. Opin. Cell Biol. **5:**48–55.
9. **Izumo, S., B. Nadal-Ginard, and V. Mahdavi.** 1988. Protooncogene induction and reprogramming of cardiac gene expression produced by pressure overload. Proc. Natl. Acad. Sci. USA **85:**339–343.
10. **Kumar, A., K. Crawford, L. Close, M. Madison, J. Lorenz, T. Doetschman, S. Pawlowski, J. Duffy, J. Neumann, J. Robbins, G. P. Boivin, B. A. O'Toole, and J. L. Lessard.** 1997. Rescue of cardiac alpha-actin-deficient mice by enteric smooth muscle gamma-actin. Proc. Natl. Acad. Sci. USA **94:**4406–4411.
11. **Kusakabe, T., I. Araki, N. Satoh, and W. R. Jeffery.** 1997. Evolution of chordate actin genes: evidence from genomic organization and amino acid sequences. J. Mol. Evol. **44:**289–298.**:**
12. **Laing, N. G., S. D. Wilton, P. A. Akkari, S. Dorosz, K. Boundy, C. Kneebone, P. Blumbergs, S. White, H. Watkins, D. R. Love, et al.** 1995. A mutation in the alpha tropomyosin gene TPM3 associated with autosomal dominant nemaline myopathy NEM1. Nat. Genet. **10:**249.
13. **Laing, N. G.** 1999. Inherited disorders of sarcomeric proteins. Curr. Opin. Neurol. **12:**513–518.
14. **Lehman, W., M. Rosol, L. S. Tobacman, and R.Craig.** 2001. Troponin organization on relaxed and activated thin filaments revealed by electron microscopy and three-dimensional reconstruction. J. Mol. Biol. **307:**739–744.
15. **Lessard, J. L.** 1988. Two monoclonal antibodies to actin: one muscle selective and one generally reactive. Cell Motil. Cytoskel. **10:**349–362.
16. **McHugh, K. M.** 1995. Molecular analysis of smooth muscle development in the mouse. Dev. Dyn. **204:**278–290.
17. **McHugh, K. M., K. Crawford, and J. L. Lessard.** 1991. A comprehensive analysis of the developmental and tissue-specific expression of the isoactin multigene family in the rat. Dev. Biol. **148:**442–458.
18. **Mogensen, J., I. C. Klausen, A. K. Pedersen, H. Egeblad, P. Bross, T. A. Kruse, N. Gregersen, P. S. Hansen, U. Baandrup, and A. D. Borglum.** 1999. Alpha-cardiac actin is a novel disease gene in familial hypertrophic cardiomyopathy. J. Clin. Investig. **103:**R39-R43.
19. **Mounier, N., and J. C. Sparrow.** 1997. Structural comparisons of muscle and nonmuscle actins give insights into the evolution of their functional differences. J. Mol. Evol. **44:**89–97.
20. **Nowak, K. J., D. Wattanasirichaigoon, H. H. Goebel, M. Wilce, K. Pelin, K. Donner, R. L. Jacob, C. Hubner, K. Oexle, J. R. Anderson, C. M. Verity, K. N. North, S. T. Iannaccone, C. R. Muller, P. Nurnberg, F. Muntoni, C. Sewry, I. Hughes, R. Sutphen, A. G. Lacson, K. J. Swoboda, J. Vigneron, C. Wallgren-Pettersson, A. H. Beggs, and N. G. Laing.** 1999. Mutations in the skeletal muscle alpha-actin gene in patients with actin myopathy and nemaline myopathy. Nat. Genet. **23:**208–212.
21. **Olson, T. M., T. P. Doan, N. Y. Kishimoto, F. G. Whitby, M. J. Ackerman, and L. Fananapazir.** 2000. Inherited and de novo mutations in the cardiac actin gene cause hypertrophic cardiomyopathy. J. Mol. Cell Cardiol. **32:** 1687–1694.
22. **Olson, T. M., V. V. Michels, S. N. Thibodeau, Y. S. Tai, and M. T. Keating.** 1998. Actin mutations in dilated cardiomyopathy, a heritable form of heart failure. Science **280:**750–752.
23. **Rubenstein, P. A.** 1990. The functional significance of multiple actin isoforms. BioEssays **2:**309–315.
24. **Ruzicka, D. L., and R. J. Schwartz.** 1988. Sequential activation of α-actin

genes during avian cardiogenesis: vascular smooth muscle α-actin gene transcripts mark the onset of cardiomyocyte differentiation. J. Cell Biol. **107:** 2575–2586.
25. **Sawtell, N. M., and J. L. Lessard.** 1989. Cellular distribution of smooth muscle actins during mammalian embryogenesis: expression of the α-vascular but not the γ-enteric isoform in differentiating striated muscle. J. Cell Biol. **109:**2929–2937.
26. **Schurch, W., O. Skalli, T. A. Seemayer, and G. Gabbiani.** 1987. Intermediate filament proteins and actin isoforms as markers for soft tissue tumor differentiation and origin. I. Smooth muscle tumors. Am. J. Pathol. **128:**91–103.
27. **Schwartz, K., D. de la Bastie, P. Bouveret, P. Oliviero, S. Alonso, and M. Buckingham.** 1986. Alpha-skeletal muscle actin mRNA's accumulate in hypertrophied adult rat hearts. Circ. Res. **59:**551–555.
28. **Shull, M. M., and T. Doetschman.** 1994. Transforming growth factor-beta 1 in reproduction and development. Mol. Reprod. Dev. **39:**239–246.
29. **Skalli, O., P. Ropraz, A. Trzeciak, G. Benzonana, D. Gillessen, and G. Gabbiani.** 1986. A monoclonal antibody against alpha-smooth muscle actin: a new probe for smooth muscle differentiation. J. Cell Biol. **103:**2787–2796.
30. **Strezelecka-Golaszewska, H., and A. Sobieszek.** 1981. Activation of smooth muscle myosin by smooth muscle and skeletal muscle actins. FEBS Lett. **134:**197–202.
31. **Sutoh, K., and I. Mabuchi.** 1984. N-terminal and C-terminal segments of actin participate in binding depactin, an actin depolymerizing protein from starfish oocytes. Biochemistry **23:**6757–6762.
32. **Vandekerckhove, J., G. Bugaisky, and M. Buckingham.** 1986. Simultaneous expression of skeletal muscle and heart actin proteins in various striated muscle tissues and cells. A quantitative determination of the two actin isoforms. J. Biol. Chem. **261:**1838–1843.
33. **Vandekerckhove, J., and K. Weber.** 1978. At least six different actins are expressed in a higher mammal: an analysis based on the amino acid sequence of the amino-terminal tryptic peptide. J. Mol. Biol. **126:**783–802.